# Methodology for the constitution of a restricted set of heatwaves, derived from climate projections, that can be used for building performance simulations

Adrien Toesca[1], Damien David[*1], Kévyn Johannes[1], and Michel Lussault[2]

*1 Univ Lyon, INSA Lyon, CNRS, CETHIL, UMR5008*
*Bâtiment Sadi-Carnot, 9, rue de la Physique, Campus LyonTech La Doua*
*69621*
*Villeurbanne cedex, France*
**Corresponding author: Damien.david@insa-lyon.fr*

*2 University of Lyon, UMR5600 EVS*
*18, rue Chevreul, 69362*
*Lyon Cedex, France*

## ABSTRACT

In the context of climate change, Building Performance Simulations are used to assess the ability of passive buildings to maintain acceptable comfort conditions, or to limit the air conditioning energy consumption during heatwaves. Climate projection data, including heatwaves, are needed to feed the Building Performance Simulation tools. A building, located in a given location, is likely to experience several heatwaves with different characteristics in the coming decades. There is a need to develop a methodology dedicated to the constitution of heatwave weather files datasets, that are representative of the local meteorological diversities, and that are sufficiently reduced to limit the number of required simulations to assess building performances. This is the objective of the 4-step methodology described in this article. The methodology is tested for the location of Lyon Saint-Exupéry airport, France. The first two steps consist in collecting climate projection data, and detecting heatwaves contained in these data. For Lyon Saint-Exupéry airport, 2384 heatwaves were detected. The last two steps consist in characterizing the heatwaves and selecting a set of distinct heatwaves, representative of the meteorological diversity of a given location. For Lyon, the methodology identified 10 distinct heatwave groups using an agglomerative hierarchical clustering method.

## KEYWORDS

Heatwaves, climate projection, summer thermal comfort, building performance simulations

## 1 INTRODUCTION

In the context of climate change, extreme weather events, such as heatwaves, will become more frequent, intense and long. Extreme temperatures cause discomfort and health issues in the outdoor and indoor environments of buildings. This is particularly true in passive buildings, which do not have active cooling systems to ensure comfortable indoor environments. According to (Santamouris, 2019), 92% of residential buildings can be considered as passive buildings for summer conditions in Europe. Energy peaks are also an issue for buildings with active cooling systems when they are subjected to heatwaves. (IEA (International Energy Agency) 2018) reported that around 2/3 of the world's buildings would be equipped with air-conditioning systems by 2050. In order to assess the ability of current passive buildings to maintain a comfortable indoor environment, or to limit the energy consumption, during future heatwaves, meteorological data representative of future extreme events is needed.

In the coming decades, it is difficult to imagine that a building in a given location will be only subjected to a single heatwave or several similar heatwaves. The building will more likely be subjected to several heatwaves, each heatwave having different characteristics. Therefore, it is not sufficient to use only one heatwave weather file to assess the future performances of buildings under such various heatwave conditions.

According to (Machard et al. 2020), the climate projection data from the CORDEX (Coordinated Regional Climate Downscaling Experiment) project is a suitable data source for constructing heatwave meteorological files for Building Performance Simulations (BPS). CORDEX is a project supervised by the World Climate Research Program (WCRP). It initially aims to compare the performance of different RCM (Regional Climate Model) simulation tools. RCM are climate models adapted to domain sizes of the order of a few thousand kilometres. Unlike GCM, their simulation domain does not cover the entire surface of the earth. RCM are used to downscale simulation data produced by GCM, which have a very coarse temporal and spatial grid. GCM and RCM simulate the interactions between the different components of the climate system (atmosphere, oceans, rivers, soil, etc.) under external forcing's such as solar radiation and greenhouse gases. The data produced by the CORDEX project are hosted on the Earth System Grid Federation (ESGF) platform, which ensures the management, dissemination and analysis of simulation data. The data currently available on this platform were obtained from the GCM results of the fifth Coupled Model Intercomparison Project (CMIP5). In the CORDEX project, the world has been divided into different geographical zones. The data resulting from these simulations are named by adding the code of the simulated area to the CORDEX term (as an example, the EuroCORDEX data for the European area). The data available are either raw simulation results, or bias-corrected simulation results. (Ouzeau et al. 2016) and (Lorenzo, Díaz-Poso, et Royé 2021) used the climate projection data from the CORDEX project to study the evolution of heatwaves over time in France and on the Iberian Peninsula respectively. Both papers show the ability of climate projection data from the CORDEX project to represent heatwaves.

The 4-step methodology proposed in the present article aimed at building representative heatwave weather datasets for a given location, and for BPS. Each section of this article details one step of the methodology described in Figure 1. The first two steps aim at building a dataset of possible future heatwaves. The objective of the last two steps is to characterise heatwaves, and based on this characterisation, to select a set of distinct heatwaves, representative of the meteorological diversity of a given location. In this paper, the methodology is applied to the location of Lyon Saint-Exupéry airport. Table 1 provides general information about the case study.

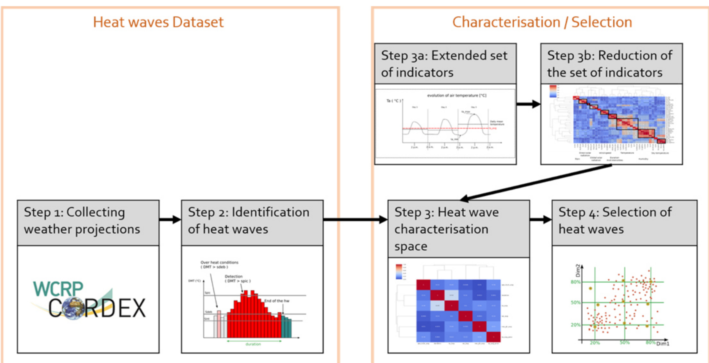


Figure 1: Scheme of the methodology

Table 1: General information on the case study

| Name | Latitude | Longitude | Altitude | Time Zone |
|---|---|---|---|---|
| Lyon-Saint-Exupéry airport, France | 45.7261<br>45° 43' 34" North | 5.09083<br>5° 5' 27" East | 250 m | UTC +1:00 (Europe/Paris)<br>Summer time: UTC +2:00<br>Winter time: UTC +1:00 |

## 2 STEP 1: COLLECTING CLIMATE PROJECTION DATA

The objective of the first step is to collect and transform meteorological data for climate projections up to 2100 from the CORDEX database, for several RCP scenarios and several models. A model is a combination of a GCM, a RCM, and an ensemble of perturbations applied to the downscaling simulations in order to assess the stability of the different RCMs. (Machard et al, 2020) has related that the variations between the future weather projections are equally due to the different RCP scenario, and to the different assumptions made by the various models. Since the purpose of the first step is to cover all the possible future weather conditions, the variability due to both models and RCP scenarios must be considered.

The weather data must contain a minimum set of variables in order to be usable as an input weather file for BPS. The minimum set of variables for a weather file type EPW (EnergyPlusWeatherFile) is describe in (U.S. Department of Energy 2021). Weather data must be in hourly time steps.

Climate projection data produced in the CORDEX project cannot be directly used in BPS. However, they can be transformed to make them exploitable in BPS, if they contain a minimum set of variables, whose data are available at a sufficiently short time step. The available CORDEX data must be filtered according to this criterion. To limit the amount of projection data to be downloaded, one additional arbitrary criterion was added: the selected weather projection had to come from models for which at least 3 projections were available, among different combinations of RCP scenario and data post-processing status (raw or bias-corrected simulation results).

Table 2 describes the minimum set of available variables, and the minimum timestep for each variable, that must be used to identify the weather projections that are adapted to BPS. It contains three additional variables compared to the minimum set of variables proposed by (Machard et al. 2020): the incident infrared radiation and the two components of the wind speed that allow the calculation of the wind direction. The minimum timestep was adjusted according to the availability of data from the CORDEX project. Most of the variables are available at a time step of 3h, except for the wind components, which are used to calculate the wind direction and are available at a timestep of 6h. Only three variables from the CORDEX project are available with a bias correction: the dry air temperature, the specific humidity, and the wind speed.

In order to bring them back to hourly time steps, interpolations have been performed. In some climatic contexts, a time step of 3 or 6 hours may not capture the relevant changes, and information may be missed through interpolation. This limitation is inherent in CORDEX data. The methodology from (Machard et al. 2020) has been used to compute the variables needed in EPW files from the EuroCORDEX climate projections.

Table 2: Minimum set variables used to filter out those climate projections that are usable for BPS

| CORDEX symbols | Variables names | Timestep | Bias-correction availability |
|---|---|---|---|
| tas | Dry air temperature [K] | 3hrs | Yes |
| huss | Specific humidity [kg/kg] | 3hrs | Yes |
| ps | Atmospheric pressure [Pa] | 3hrs | - |
| clt | Cloud fraction [%] | 3hrs | - |
| rsds | Global horizontal radiation [W/m²] | 3hrs | - |
| sfcwind | Wind speed [m/s] | 3hrs | Yes |
| pr | Precipitation [kg/m²/s] | 3hrs | - |
| rlds | Surface Downwelling Longwave Radiation [W/m²] | 3hrs | - |
| uas | Eastward wind speed [m/s] | 6hrs | - |
| vas | Northward wind speed [m/s] | 6hrs | - |

Table 3 details the 44 selected climate projections that were collected for the case study of the Lyon Saint-Exupéry airport location. Each climate projection covers the period between 2007 and 2097. So, the collected data represent a total of 3960 simulated years. Those data were produced by 11 different climate projection models (GCM+RCP+ensemble of perturbations). Of these 44 results, 14 are bias-corrected data and 30 are raw simulation results.
The entire data selection and collection process has been automated with a python routine. The python library "pyesgf" was used to access to the CORDEX database, hosted by ESGF. Then the python library "xarray" was used to perform a remote selection of the data corresponding to the localisation of the Lyon-Saint-Exupéry airport. The use of the "xarray" library reduced significantly the volume of data that needed to be downloaded.

Table 3: List of the climate projection results collected for this study. Crosses indicate data availability.

| **Models** | | | **Raw data** | | | **Bias-corrected data** | |
|---|---|---|---|---|---|---|---|
| **GCM** | **RCM** | **Ensemble** | **rcp26** | **rcp45** | **rcp85** | **rcp45** | **rcp85** |
| CNRM-CERFACS-CNRM-CM5 | ALADIN63 | r1i1p1 | X | X | X | | |
| CNRM-CERFACS-CNRM-CM5 | RAMCO22E | r1i1p1 | X | X | X | | |
| CNRM-CERFACS-CNRM-CM5 | RCA4 | r1i1p1 | | X | X | X | X |
| ICHEC-EC-EARTH | RAMCO22E | r1i1p1 | | X | X | X | X |
| IPSL-IPSL-CM5A-MR | RCA4 | r1i1p1 | | X | X | X | X |
| MOHC-HadGEM2-ES | RAMCO22E | r1i1p1 | X | X | X | X | X |
| MOHC-HadGEM2-ES | RCA4 | r1i1p1 | X | X | X | X | X |
| MPI-M-MPI-ESM | RCA4 | r1i1p1 | X | X | X | X | X |
| NCC-NorESM1-M | RCA4 | r1i1p1 | X | X | X | | |
| ICHEC-EC-EARTH | RAMCO22E | r12i1p1 | X | X | X | | |
| ICHEC-EC-EARTH | RCA4 | r12i1p1 | X | X | X | X | X |

# 3 STEP 2: IDENTIFYING HEATWAVES

The objective of this step is to identify heatwaves contained in the collected climate projection data. There is no universal definition of what is a heatwave. Four methods of heatwave detection are commonly referred to: the "Spic, Sdeb, Sint" method from (Ouzeau et al. 2016), the "IBM" method from (Pascal et al. 2006), the "EHF" method from (Nairn et Fawcett 2014) and the "HWMI" method from (Russo et al. 2014).
In order to avoid redundancy within the heatwave dataset, only one heatwave detection method must be retained. For the same reason, a choice has to be made between raw simulation data and bias corrected simulation data. The objective of the methodology is to produce weather data that represent severe weather conditions. So, the retained heatwave detection method and post-processing status must be the pair that detect the most severe set of heatwaves.
Table 4 shows the average annual number (frequency), the average air temperature and the average duration of heatwaves per simulation data post-processing status, detected with each of the four heatwave detection methods for the case study of Lyon Saint-Exupéry airport. The statistics contained in the Table 4 are used to select the appropriate heatwave detection method and weather data post-processing status.
The number of heatwaves detected in the bias-corrected climate projection data is greater than the number of heatwaves detected in the raw data. Without the bias correction, the temperatures in the CORDEX projections seems to be underestimated, resulting in a lower number of heatwaves. The heatwave dataset will therefore be constituted of the heatwaves detected on the bias-corrected climate projection data
The "EHF" and "HWMI" methods detect significantly more heatwaves than the other two methods. Those methods detect many heatwaves outside the summer period: heatwaves detected during May and September represent 22% and 35% of the total heatwaves detected by respectively the "EHF" method and the "HWMI" method. Therefore, the average air

temperatures during heatwaves of "EHF" and "HWMI" methods are more than 3°C lower than the average temperatures obtained with the other two methods. For this study, we intend to keep only the hottest heatwaves. For that reason, the “EHF” method and the “HWMI” method are not retained.
There is a 90% correspondence between the heatwave periods detected with the "IBM" method and the "Spic, Sdeb, Sint" method. However, heatwaves identified with the "Spic, Sdeb, Sint" method are 8 days longer and 2°C cooler on average than the ones detected by the “IBM” method, as shown in the histograms in Figure 2. The “IBM” method identifies the core of the heatwaves, which is why they are warmer and shorter on average. The histogram on the left shows that the durations defined by the “Spic, Sdeb, Sint” method are more staggered. As the staggered durations will make it easier to distinguish between the different heatwaves, the "Spic, Sdeb, Sint" method was selected.

Table 4: Average annual number, air temperature and duration of heatwaves per simulation data post-processing status detected from each detection method.

| Detection methods | Raw data | | | Bias-corrected data | | |
|---|---|---|---|---|---|---|
| RCP | Average annual number of heatwaves | Average air temperature | Average duration | Average annual number of heatwaves | Average air temperature | Average duration |
| Spic, Sdeb, Sint | 0.80 | 28.12 °C | 12.6 d | 1.89 | 28.3°C | 14.5 d |
| IBMn, IBMx | 0.77 | 29.8 °C | 5.9 d | 1.77 | 30.3°C | 6.3 d |
| EHF | 3.57 | 24.5 °C | 9.1 d | 6.06 | 24.8°C | 11.1 d |
| HWMI | 2.99 | 25.4 °C | 6.3 d | 6.65 | 25.6°C | 6.9 d |

At the end of step 2, the heatwave dataset consists of 2384 heatwaves, detected by the “Spic, Sdeb and Sint” method from (Ouzeau et al. 2016), for the location of Lyon Saint-Exupéry airport. This data is derived from the bias-corrected climate projection data (green cells in Table 4). Please note that the selection of bias corrected data induced a restriction to the RCP45 and the RCP85 scenario, no bias corrected data were made available for the RCP26 scenario.

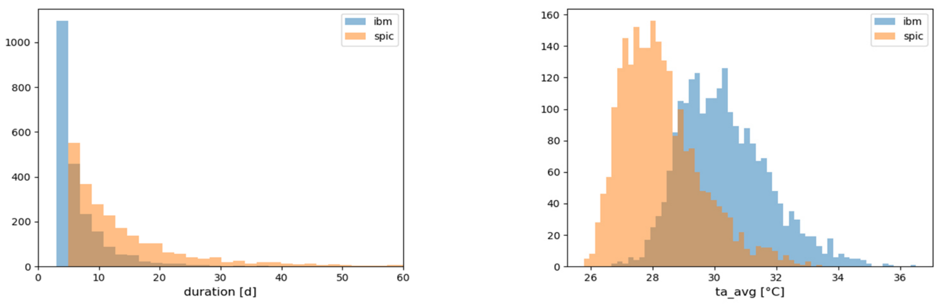


Figure 2: Histograms of the durations (left) and average temperatures (right) of the heatwaves detected by the 'ibm' (blue) and 'Spic, Sdeb, Sint' (orange) methods

## 4 STEP 3: CHARACTERISING HEATWAVES

The objective of this step is to define a restricted set of indicators that characterize the different heatwaves stored in the heatwave dataset.
The indicators of the restricted set of indicators will constitute the dimensions of a heatwave characterisation space, in which representative heatwaves will be selected during the step four. This restricted set of indicators must be sufficiently diversified to cover all the characteristics of the detected heatwaves, but small enough to limit the number of dimensions of the characterisation space from which the heatwaves will be selected.

An extended set of indicators is first arbitrarily established in the step 3a. Then this set of indicators is reduced to a minimum by keeping only independent and significant indicators using statistical methods in the step 3b.

## 4.1 Step 3a: Constitution of the extended set of indicators

The extended set of indicators consists, first of all, of statistical quantities calculated on the available meteorological data (air temperature, global solar radiation, etc.) during the period of the heatwaves: the average value (avg), the maximum value (max), the minimum value (min), the average daily amplitude value (dampl_avg), the average of the daily minimum and maximum values (dmin_avg/dmax_avg), and the night-time and daytime averages (nighttime/daytime). The extended set of indicators also contains the heatwave intensity indicators defined by (Ouzeau et al. 2016), (Nairn et al. 2014) and (Russo et al. 2014). Those indicators are named intensity_spic, intensity_ehf, and intensity_hwmi respectively.
Other specific indicators have been developed to quantify the cooling opportunities of building during the heatwaves. Those indicators are called cooling potential indicators. Their definitions are represented schematically in the Figure 3. The cooling potential indicators correspond to the areas under the curves (in blue for the cooling potential by evaporation, in orange for the cooling potential by thermal radiation, in yellow for the cooling potential by solar protection, and finally in grey for the cooling potential by natural ventilation), divided by the heatwave duration, in days unit. The list of the extended set of indicators is shown along the axes of the matrix displayed in Figure 4. The value of each of those indicators was calculated for the 2384 collected heatwaves.

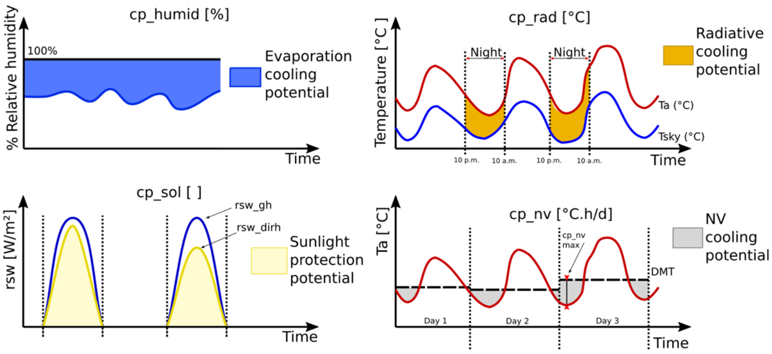


Figure 3: Cooling potential (by evaporation top left, by direct radiation protection bottom left, by night-time heat radiation top right and by natural ventilation bottom right)

## 4.2 Step 3b: Reduction of the set of indicators

The heatwave indicators will be used in step 4, to rank the heatwaves according to the characteristics they measure, and then to select a restricted set of heatwaves based on the rankings. Two indicators are correlated when the rankings from these two indicators are very similar. In this case, the information provided by the second indicator is redundant with information already provided by the first indicator. On the other hand, two indicators are independent when the rankings of the two indicators are very different. In this case, the information provided by the second indicator is of real interest since it allows to distinguish a new characteristic of the heatwaves.
The first objective of step 3b is to reduce the extended set of indicators to a set of independent indicators. For this purpose, the clustering method has been considered. This method is applied on a dataset containing the values of all the indicators contained in the extended set of indicators, for all the collected heatwaves.
The method consists in clustering the indicators, with the absolute value of the Pearson correlation as the clustering metric. Figure 4 shows the matrix of correlation between all indicators of the extended set of indicators. The arrangement of the indicators is the result of

the application of the UGPMA (Unweighted Pair Group Method with Arithmetic mean) hierarchical agglomerative classification method. The dendrogram above and on the left of the matrix shows a hierarchy of the groups of indicators according to their degree of dependence.
Groups of indicators have been defined arbitrarily from the classification provided by the UGPMA algorithm. Those groups are delimited by thick line rectangles within the correlation matrix displayed on Figure 4. In fact, it turned out that the UPGMA algorithm clustered the indicators around their associated meteorological quantity (temperature, humidity, solar radiation, wind, rain, etc.). Thus, it was decided to locate the limits of the groups of indicators at the transitions between the various associated meteorological quantities. For ease of identification, a name has been given to each group, and those names are shown at the bottom of the matrix.
Most of the cooling potential indicators are placed in groups that correspond to their associated meteorological quantity. For example, the evaporative cooling potential ("cp_humid") is highly corelated with the relative humidity, so it belongs to the same group. The cooling potential by protection against direct solar radiation ("cp_sol") is grouped with the solar radiation quantities. However, the sky temperature and the humidity groups are distinct groups but both quantities are linked together by the average specific humidity, that is highly correlated either with the average relative humidity and with the sky temperature. This relationship between the humidity and the sky temperature explains why the radiative cooling potential ("cp_rad") belongs to the humidity group, even if it is computed from the sky temperature.
The intensity of heatwaves defined by (Ouzeau et al. 2016) and (Russo et al. 2014) ("intensity_spic" and "intensity_hwmi") are correlated with the duration of heatwaves rather than the air temperature from which they are computed. This is because those indicators are cumulative: the longer is the heatwave, the higher is the value of the indicator. They measure more the duration of the heatwave than the instantaneous severity of the weather conditions.
In order to reduce the extended set of indicators to a set of independent indicators, only one indicator was kept in each group. The list of independent indicators resulting for that selection is given in Table 5. This selection was done in an arbitrary way, but followed a logic: as soon as it was possible, the average value of the selected weather quantity was chosen, to facilitate the interpretation of the results. Average specific humidity is selected as the representative indicator of both humidity and sky temperature groups, since both groups are well correlated. For the same reason, the average horizontal global solar radiation has been retained to represent both solar radiation groups.
The second objective of step 3b is to further reduce the selected set of indicators to meaningful indicators. A meaningful indicator is an indicator that represent a characteristic of the heatwaves that varies sufficiently among the dataset to produce significant changes on the building thermal solicitations. Table 5 shows the minimum and maximum value of each independent indicator. Some of the independent indicators are not kept (red rectangle on the Figure 4) because they correspond to quantities that would have very little influence on the thermal behaviour of buildings, they are not meaningful. This is the case for the "rain" group. Precipitation is low and is therefore not responsible for a drop-in temperature. According to MétéoFrance, a rainfall can be considered as light rain when its intensity is less than 3 mm/h. Figure 5 shows the histogram of the maximum precipitation (left) during heatwaves, it appears that most of the maximum precipitation are below 3 mm/h. The minimum temperature is mainly during the first day of the detected heatwaves and is due to the detection method. The main wind direction is also not meaningful. There are only two main directions, that are shown by the histogram in Figure 5: North and South. There is almost no influence of wind for mono-oriented building, but there is an influence of the wind direction for cross-ventilated building. In the case of Lyon, the two major directions are symmetrical so the influence on cross-ventilated building will be the same if the wind come from North or South. The main wind direction during heatwaves is

then not retained for the rest of the study. Heatwaves can therefore be characterised by a space composed of 6 dimensions, represented by the indicators listed in bold in Table 5.

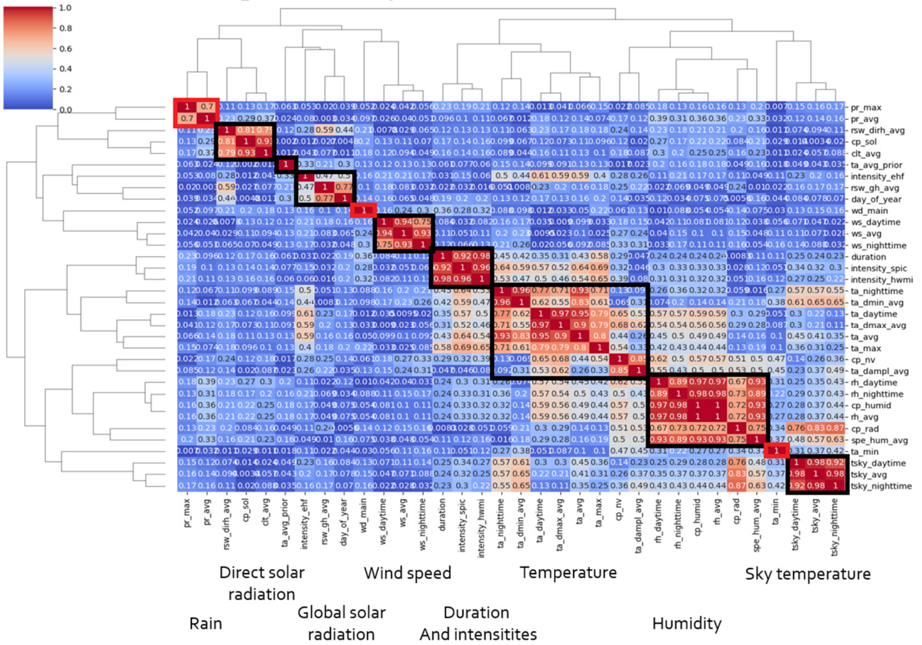


Figure 4: Correlation matrix (in absolute values) between the different indicators characterising heatwaves. Strong correlations are shown in red, and weak ones in blue. At the bottom of the figure, the groups of indicators that are highly correlated are shown.

Table 5: Minimum and maximum value of each independent indicator. The independent and meaningful indicators are written in bold.

| Indicator | Variable name | Unity | Minimum | Maximum |
|---|---|---|---|---|
| Average rain quantity | pr_avg | mm/h | 0 | 0.46 |
| Minimum temperature | ta_min | °C | 12.0 | 22.9 |
| **Average temperature** | ta_avg | °C | 25.8 | 33.4 |
| **Duration** | duration | Days | 5 | 100 |
| Main wind direction | wd_main | ° | 0 | 337.5 |
| **Average wind speed** | ws_avg | m/s | 1.3 | 6.2 |
| **Average horizontal global solar radiation** | rsw_gh_avg | W/m² | 143.5 | 347.9 |
| **Average specific humidity** | spe_hum_avg | gv/kg | 4.7 | 15.9 |
| **Average temperature before the heatwave** | ta_avg_prior | °C | 15.6 | 30.9 |

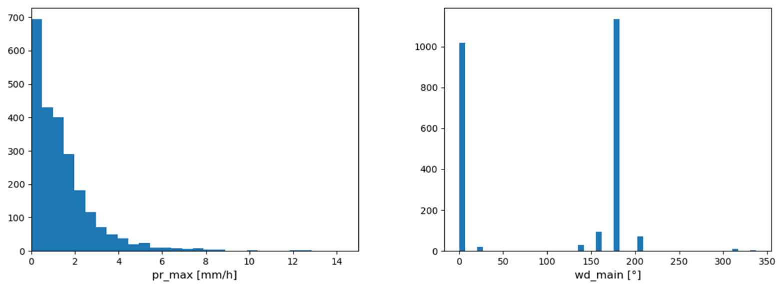


Figure 5: Histograms of the maximum precipitation (left) and main wind directions (right) of the heatwave dataset

## 5 STEP 4: SELECTING HEATWAVES

The heatwave dataset from step 2 contains 2384 heatwaves. The last step of the methodology aims at selecting, from this large number of heatwaves, a reduced set of distinct heatwaves, representative of the diversity of the heatwaves contained in the whole dataset.

The selection is performed on the characterization space whose dimensions are made of the restricted set of indicators produced by step 3.

An agglomerative hierarchical clustering method is used. In this method, each heatwave is first considered as a single cluster, making the total number of clusters equal to the number of heatwaves. Then heatwaves are grouped together based on similarity metrics, computed on the 6 dimensions of the characterization space, creating clusters as one moves up the hierarchy. In this study, the metric is computed with Euclidean distance and the "Ward" linkage method from the scipy.cluster.hierarchy.linkage python library is used to select the closest clusters. "Ward" linkage method uses the Ward variance minimization algorithm. This approach is iterative and is also called a bottom-up approach. At each iteration, the distance matrix between each cluster is calculated and the two closest clusters are grouped together and so on. In the end, the data is all grouped into a single cluster. With this method, it is possible to draw a dendrogram.
A dendrogram is a tree diagram that illustrates the arrangement of clusters produced by the corresponding analyses. Figure 6 shows the dendrogram obtained for the dataset of heatwaves. The samples on the x-axis are arranged automatically, representing very close points that will remain closer to each other. The length of the branches of the dendrogram (y-axis) indicates the distance between two clusters, so it is possible to use this distance to choose the final number of clusters. The number of clusters retained for this study is chosen arbitrarily. In this study, 10 clusters are retained. They are represented with different colours in Figure 6. Figure 6 shows also with a black horizontal line (left graph), where it was decided to cut the dendrogram to select the number of clusters.  This number of clusters allows to obtain distinct heatwave groups. If less clusters were kept, the data inside each cluster would have been further from each other. The Euclidean distance is indeed increasing a lot with less than 10 clusters. At the end, only the closest heatwave from the barycentre of each cluster is selected.

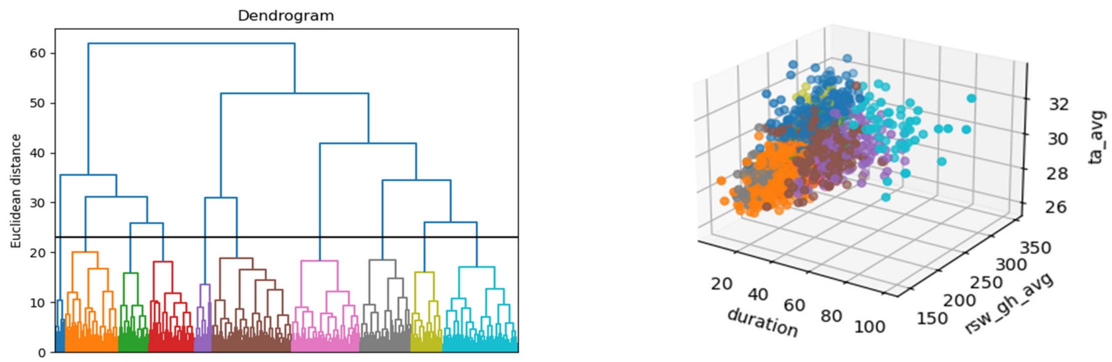


Figure 6: dendrogram of the heatwave dataset in the characterisation space (left) and 3D representation of the heatwave dataset with duration, average global horizontal solar radiation and average air temperature dimensions

Figure 6 shows, on the right graph, a 3D representation of the heatwave dataset with the use of the following dimensions: duration, average global horizontal solar radiation and average air temperature. This view is limited because it does not distinguish the 6 dimensions of the characterisation space, but it still allows to visualize different clusters. As an example, the light blue cluster represent long, warm heatwaves with a lot of solar radiation.

## 6 CONCLUSIONS

The methodology developed in this paper allows the construction of meteorological projection files containing distinct heatwaves that can be used for building performance simulations. A heatwave characterisation space composed of significant and independent meteorological indicators has been created, allowing to identify 10 different heatwave groups out of the 2384 heatwaves detected for the location of Lyon Saint Exupéry airport. This number is low enough to allow BPS to be carried out for each of the most representative heatwave of each cluster. It will therefore be possible to study the capacity of buildings to maintain acceptable comfort conditions during future heatwaves. In particular, it will be possible to study the effectiveness of cooling by natural ventilation. Are passive techniques effective enough or is the use of air conditioning essential?

## 7 ACKNOWLEDGEMENTS

We gratefully acknowledge the Convergence Institute Lyon Urban School (LUS) for funding the research described in this paper.
We acknowledge the World Climate Research Program's Working Group on Regional Climate, and the Working Group on Coupled Modelling, former coordinating body of CORDEX and responsible panel for CMIP5. We also thank the climate modelling groups (listed in Table 3 of this paper) for producing and making available their model output. We also acknowledge the Earth System Grid Federation infrastructure an international effort led by the U.S. Department of Energy's Program for Climate Model Diagnosis and Intercomparison, the European Network for Earth System Modelling and other partners in the Global Organisation for Earth System Science Portals (GO-ESSP).

## 8 REFERENCES

IEA (International Energy Agency). 2018. « The Future of Cooling: Opportunities for energy-efficient air conditioning | READ online ». oecd-ilibrary.org. 2018. https://read.oecd-ilibrary.org/energy/the-future-of-cooling_9789264301993-en.

Lorenzo, Nieves, Alejandro Díaz-Poso, et Dominic Royé. 2021. « Heatwave Intensity on the Iberian Peninsula: Future Climate Projections ». *Atmospheric Research* 258 (août): 105655. https://doi.org/10.1016/j.atmosres.2021.105655.

Machard, Anaïs, Christian Inard, Jean-Marie Alessandrini, Charles Pelé, et Jacques Ribéron. 2020. « A Methodology for Assembling Future Weather Files Including Heatwaves for Building Thermal Simulations from the European Coordinated Regional Downscaling Experiment (EURO-CORDEX) Climate Data ». *Energies* 13 (13): 3424. https://doi.org/10.3390/en13133424.

Nairn, John, et Robert Fawcett. 2014. « The Excess Heat Factor: A Metric for Heatwave Intensity and Its Use in Classifying Heatwave Severity ». *International Journal of Environmental Research and Public Health* 12 (1): 227-53. https://doi.org/10.3390/ijerph120100227.

Ouzeau, G., J. -M. Soubeyroux, M. Schneider, R. Vautard, et S. Planton. 2016. « Heat Waves Analysis over France in Present and Future Climate: Application of a New Method on the EURO-CORDEX Ensemble ». *Climate Services* 4 (décembre): 1-12. https://doi.org/10.1016/j.cliser.2016.09.002.

Pascal, Mathilde, Karine Laaidi, Martine Ledrans, Elsa Baffert, Céline Caserio-Schönemann, Alain Le Tertre, Jacques Manach, Sylvia Medina, Jérémie Rudant, et Pascal Empereur-Bissonnet. 2006. « France’s Heat Health Watch Warning System ». *International Journal of Biometeorology* 50 (3): 144-53. https://doi.org/10.1007/s00484-005-0003-x.

Russo, Simone, Alessandro Dosio, Rune G. Graversen, Jana Sillmann, Hugo Carrao, Martha B. Dunbar, Andrew Singleton, Paolo Montagna, Paulo Barbola, et Jürgen V. Vogt. 2014. « Magnitude of Extreme Heat Waves in Present Climate and Their Projection in a Warming World ». *Journal of Geophysical Research: Atmospheres* 119 (22): 12,500-12,512. https://doi.org/10.1002/2014JD022098.

Santamouris, Mat. 2019. *Cooling Energy Solutions for Buildings and Cities*. WORLD SCIENTIFIC. https://doi.org/10.1142/10901.

U.S. Department of Energy. 2021. « EnergyPlus Version 9.6.0 Documentation - Auxiliary Programs », septembre, 257.